

Understanding Signal Sources of MT Asymmetry and Inhomogeneous MT for Imaging Myelination

Jae-Woong Kim¹, Seung Hong Choi², and Sung-Hong Park¹

¹Korea Advanced Institute of Science and Technology, Daejeon, Korea, ²Seoul National University, Seoul, Korea

Introduction : Myelin is an essential component to normal brain function. To image myelination, various MRI techniques have been developed including myelin water imaging (1). Recently, techniques based on asymmetric aspects of magnetization transfer (MT) spectrum were proposed for imaging myelination: Inhomogeneous MT (IHMT) method uses inhomogeneously broadened MT spectrum (2, 3) and MT asymmetry (MTA) utilizes the shift of MT spectrum relative to the free water peak (4). MTA can be imaged efficiently by interslice MTA using alternate ascending/descending directional navigation (ALADDIN) (5,6). In this study, we investigated the similarities and differences between MTA and IHMT at various scan conditions including the shifts in MT spectrum of various materials.

Material and Methods : The experiments were performed on a 3T Siemens Tim Trio MRI system (Siemens, Erlangen, Germany). A phantom and brain of a volunteer subject were examined. The phantom contained various materials (Fig. 1), including hair conditioners representing lamellar structure of myelin (2). Balanced steady state free precession (bSSFP) was used as data readout for all IHMT and MTA. The common imaging parameters for the bSSFP readout were TR/TE = 4.15/2.075 ms, FOV = 220x220 mm², matrix size = 128x128, slice thickness = 5 mm, and flip angle = 60°. MT saturation was conducted with 0.94μT of B₁ average value, and offset frequency (f) of 3200Hz corresponding to 25.1ppm, which were common in all IHMT and MTA. For conventional MTA and IHMT, two different types of Gaussain-shaped multiple short RF pulses were applied: one with both RF duration and inter-pulse interval of 20 ms (**Protocol A**) and the other with 5 ms (**Protocol B**), both of which had the same total saturation duration of 3 s. The conventional MTA and IHMT images were acquired on a single slice through 4 different saturation schemes in the sequence of saturation offset frequencies of (i) +f, +f, ..., (ii) +f, -f, +f, -f, ..., (iii) -f, -f, ..., and (iv) -f, +f, -f, +f, ..., as described previously (3). The acquisitions with the four schemes were repeated 8 times, yielding the total scan time of 4.4 min, and then the images were averaged for better signal to noise ratio. The datasets of (i) and (iii) were combined to generate the conventional MTA and all the four datasets of (i)–(iv) were combined for IHMT (2, 3). These data acquisition and reconstruction were repeated by asymmetrically shifting the the saturation offset frequency (Δf) in the amount of -600, -300, 0, 300 Hz, i.e., the saturation offset frequencies of $f + \Delta f$ and $-f + \Delta f$. The inter-slice ALADDIN MTA imaging was performed as described previously (5), with imaging parameters of number of slices = 19, gap = 7 mm, and scan time = 3.4 min. The intensity of WM and GM was calculated as an average values within ROIs manually defined using MATLAB.

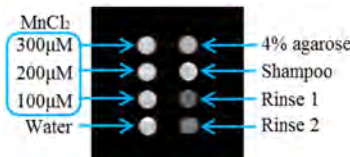


Fig. 1. Baseline image of phantom including various materials.



Fig. 2. The resulting images of conventional MTA and IHMT. The red rectangle highlights the images with negative MTA signals. Saturation RF duration = 5 ms (A) and 20 ms (B).

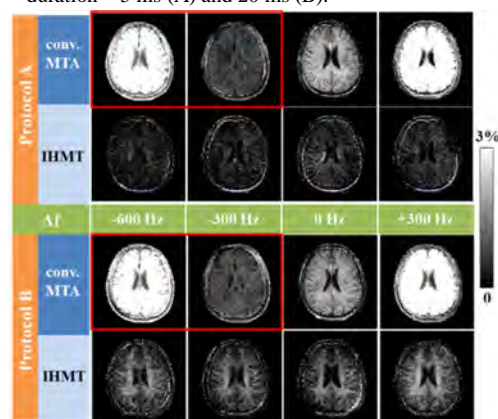


Fig. 3. The images from a normal volunteer.

Results and Discussion : When $\Delta f = 0$ Hz, conventional MTA and IHMT provided similar results showing relatively low signals in the agarose phantom but high signals in the hair conditioners, indicating high specificity to myelination (the third column in Fig. 2). However, MTA and IHMT showed different patterns depending on shifts in MT offset frequencies and saturation RF duration. MTA showed strong dependence on shifts in MT offset frequencies, whereas no dependence on the saturation RF duration (Fig. 2). To the contrary, IHMT showed strong dependence on the saturation RF duration, while almost no dependence on the shifts in MT offset frequencies (Fig. 2). Source of this observation is not clear. Note that the average saturation power and total saturation duration were the same for the saturation duration-dependent experiments (i.e., Protocols A and B). Results similar to those of the phantom were observed in the *in vivo* brain (Fig. 3). When there was no shift in MT spectrum ($\Delta f = 0$ Hz), inter-slice ALADDIN MTA showed results similar to those of conventional MTA and IHMT (Fig. 4). Quantitative results for the *in vivo* brain are summarized in Tables 1 and 2 for the case of Protocol B (RF duration = 5 ms) (Quantitative results for Protocol A is not shown, because IHMT showed little signals and MTA showed almost the same results as those of Protocol B). Under the scan conditions in this study, MTA showed higher percent signal changes but lower WM/GM ratio than IHMT (Tables 1 and 2), indicating higher sensitivity and lower specificity than IHMT.

One half of the dry weight of WM is composed of myelin and about 80% of myelin is composed of lipid (7, 8). The lipid causes shifts in MT spectrum, which may account for the specificity of MTA to myelin. ALADDIN is an efficient way of imaging MTA in multiple slices. Since sensitivity and specificity of MTA and IHMT depend on the shift in MT spectrum and the RF duration, respectively, further studies are necessary to understand the signal sources and sensitivity/specificity of MTA and IHMT for imaging myelination under various conditions.

References : 1. Kolind et al, Magn Reson Med 2009;62:106-115. 2. Varma et al, Magn Reson Med 2014. 3. Girard et al, Magn Reson Med 2014. 4. Kim et al, ISMRM 2013;Abstract #3168. 5. Park and Duong, Magn Reson Med 2011;65:1578-1591. 6. Park et al, Magn Reson Med 2012;68:1600-1606. 7. Baumann et al, APS, 2001;81:871-927. 8. O'Brien et al, J. Lipid Res 1965;6:537-544.

| | | | Δf | | | |
|------------|-----------|---------|------------|---------|------|---------|
| | | | -600 Hz | -300 Hz | 0 Hz | +300 Hz |
| Protocol B | conv. MTA | WM (%) | -3.7 | -0.9 | 1.9 | 4.9 |
| | | GM (%) | -2.8 | -0.7 | 1.2 | 3.3 |
| | | WM / GM | 1.3 | 1.2 | 1.5 | 1.5 |
| | IHMT | WM (%) | 1.5 | 1.4 | 1.4 | 1.8 |
| | | GM (%) | 0.5 | 0.4 | 0.4 | 0.6 |
| | | WM / GM | 3.2 | 3.6 | 3.2 | 2.9 |

Table 1. The percent signal of conventional MTA and IHMT on various offset frequency conditions and WM to GM ratio of intensity. Only result of protocol B is presented because IHMT signal is almost zero on protocol A.

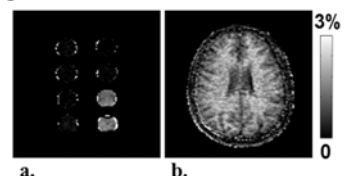


Fig. 4. Interslice MTA images obtained from ALADDIN method. a. Phantom. b. Normal brain

| | | |
|----------------|---------|-----|
| Interslice MTA | WM (%) | 2.0 |
| | GM (%) | 1.0 |
| | WM / GM | 2.1 |

Table 2. The percent signal of interslice MTA from ALADDIN acquisition. $\Delta f = 0$ Hz.